Direct current plasma jet at atmospheric pressure operating in nitrogen and air

X. L. Deng, A. Yu. Nikiforov, P. Vanraes, and Ch. Leys

Citation: J. Appl. Phys. **113**, 023305 (2013); doi: 10.1063/1.4774328
View online: http://dx.doi.org/10.1063/1.4774328
View Table of Contents: http://jap.aip.org/resource/1/JAPIAU/v113/i2
Published by the American Institute of Physics.

Direct current plasma jet at atmospheric pressure operating in nitrogen and air

X. L. Deng,[1,2] A. Yu. Nikiforov,[1,3,a)] P. Vanraes,[1] and Ch. Leys[1]
[1]*Department of Applied Physics, Ghent University, Jozef Plateaustraat 22, B-9000 Ghent, Belgium*
[2]*College of Optoelectric Science and Engineering, National University of Defense Technology, Changsha, Hunan 410073, China*
[3]*Institute of Solution Chemistry RAS, Academicheskaya str, 1, 153045 Ivanovo, Russia*

(Received 5 November 2012; accepted 18 December 2012; published online 11 January 2013)

An atmospheric pressure direct current (DC) plasma jet is investigated in N_2 and dry air in terms of plasma properties and generation of active species in the active zone and the afterglow. The influence of working gases and the discharge current on plasma parameters and afterglow properties are studied. The electrical diagnostics show that discharge can be sustained in two different operating modes, depending on the current range: a self-pulsing regime at low current and a glow regime at high current. The gas temperature and the N_2 vibrational temperature in the active zone of the jet and in the afterglow are determined by means of emission spectroscopy, based on fitting spectra of N_2 second positive system ($C^3\Pi$-$B^3\Pi$) and the Boltzmann plot method, respectively. The spectra and temperature differences between the N_2 and the air plasma jet are presented and analyzed. Space-resolved ozone and nitric oxide density measurements are carried out in the afterglow of the jet. The density of ozone, which is formed in the afterglow of nitrogen plasma jet, is quantitatively detected by an ozone monitor. The density of nitric oxide, which is generated only in the air plasma jet, is determined by means of mass-spectroscopy techniques. © *2013 American Institute of Physics*. [http://dx.doi.org/10.1063/1.4774328]

I. INTRODUCTION

Non-thermal atmospheric pressure plasma sources are of primary interest in various technological applications because of their ability to generate a high flux of different active species. With the advantage of elimination of vacuum equipment and the easy implementation in industry, atmospheric pressure plasmas can be applied in gas cleaning, film deposition, and polymer modification.[1–3] There are various methods to generate atmospheric pressure plasmas, such as microwave discharge, radio frequency discharge, dielectric barrier discharge, or direct current (DC) discharge. Recently, a lot of attention has been paid to plasma jet systems where discharge is produced with longitudinal gas flow and characterized by a long afterglow, which can be used in biomedical applications or surface modification.[4,5] In order to prevent overheating of the treated sample and constriction of the discharge, helium or argon gas is used for plasma generation. However, expensive inertial working gases (such as helium and argon) limit many practical applications of plasma jet systems. Therefore, an approach to generate non-thermal plasma with nitrogen or air is attractive. The drawback of the N_2 or air plasma is a transformation of the glow or filamentary discharge in to high current arc which should be restrained in order to keep the system at low temperature. One method to stabilize plasma is decreasing the heating instability of the discharge by a high gas flow.[6,7] Most important species generated in a nitrogen plasma and an air plasma with a long life time are various N_2 metastables, nitric oxide (NO), nitrous oxide (N_2O), ozone (O_3), atomic oxygen (O), and singlet oxygen ($^1O_2$).[8] Nitrogen metastables and $^1O_2$ can be utilized in biomedicine for bacteria killing and sterilization[9,10] because of the high energy of those excited species. NO and O_3 are of the interest for medical treatment, for example, in ozone and NO therapies.[11] NO is an important molecule regulating various processes in human skin physiology.[12] In human body mainly three processes, so called nitric-oxide-synthases (NOS), are responsible for NO generation through oxidation of L-argine to NO and L-cutrulin.[13] It is suggested in many researches that the modulation of NO availability (e.g., by NO therapies) can be the way to treat many diseases. Unfortunately, the use of NO gas for medical purposes has a number of issues, for example, NO production is difficult and expensive and NO storage has to follow strong restriction rules due to its high toxicity. The way to overcome such problems is to generate NO and other active species directly during treatment, locally and in safe level concentrations. Based on medical results, it is proved that the required density of NO during medical treatment,[14] i.e., the threshold to reach a medical, has to be around $10^{19}\,m^{-3}$, and the O_3 density has to be kept at lower level of $10^{18}\,m^{-3}$ when the medical effect of ozone is still observed and no drawbacks are presented due to the high toxicity of O_3. The use of N_2 or air plasma in glow like mode has been discussed by many groups, e.g., Akishev *et al.*[15–17] where the role of different discharge parameters on the plasma stability has been checked and analyzed. In the present study, a stable atmospheric pressure DC discharge has been obtained by using a high gas flow and a high ballast of the DC power supply. Based on results of our previous experiments[6] and data,[15,16] the ballast resistance of the

a)Author to whom correspondence should be addressed. Electronic mail: Anton.Nikiforov@Ugent.be.

discharge is fixed at 880 kΩ and the gas flow rate is maintained at 8 slm (standard liter per minute). This paper deals with a DC plasma jet used as a low temperature source of NO, O_3, and N_2 metastables when operated with pure nitrogen or dry air. The active zone and afterglow of the discharge are characterized in terms of electrical parameters, gas temperature, N_2 vibrational temperature, and species production for plasma medicine as a targeting application.

II. EXPERIMENTAL SETUP

The atmospheric pressure DC plasma jet is schematically shown in Fig. 1. The plasma is generated between pin to mesh electrodes inside a quartz tube with an inner diameter of 5 mm. The distance between the pin and the mesh is 14 mm. The anode is made of a fine-meshed metallic grid and placed at the tube outlet. The cathode, which is manufactured from a 2 mm tungsten rod with a conically sharpened tip, is connected to the negative polarity of a direct current high voltage power supply through a ballast resistor (880 kΩ). The discharge current varies from 5 to 30 mA. The flow rate of nitrogen or dry air is controlled by a MKS controller, MKS PR4000. The gas flow of the jet is maintained at 8 slm (standard liter per minute) which corresponds to a flow velocity of 6.7 m s^{-1}. The current and discharge voltage are recorded by means of a Tektronix TDS 200 digital oscilloscope with a high voltage probe P6015A. A shunt resistor (100 Ω) is used to measure the electrical current of the system. The optical emission spectrum is collected through fiber optics connected to spectrometers. The overview spectra of discharge and afterglow are recorded using an Avantes spectrometer (AvaSpec-2048, 250–800 nm, resolution 0.5 nm). The high resolution spectra in the range of 300–350 nm are obtained with another Avantes spectrometer (AvaSpec-3048, resolution 0.05 nm). Both optical systems are calibrated with a tungsten ribbon lamp and the instrumental function is obtained with an Ar pen-Ray low pressure lamp. The ozone generation in the afterglow of the discharge is obtained with an ozone monitor (Envitec, model 450). The axial distribution of ozone in the afterglow of air and N_2 is detected by changing the distance between the monitor inlet and the anode. The spatial resolution of the system is limited by the size of the inlet and estimated to be 1 mm. Generation of NO by the plasma is measured by a quadrupole mass-spectrometer (Hiden HAL/3F-RC) with a homemade atmospheric pressure inlet system. First stage of the mass-spectrometer inlet system is a capillary that determines the spatial resolution of the measurements of 1.6 mm. The main limitation of the mass-spectroscopy system with a capillary inlet is a capability to measure only neutral species with long life time. As indicated by others, the afterglow of the N_2 and air plasmas consists of atomic oxygen and nitrogen (O, N), electronic excited oxygen and nitrogen metastables (such as $O_2(a^1\Delta)$, $O_2(b^1\Sigma)$, $N_2(A^3\Sigma)$, $N_2(B^3\Pi)$, $N_2(C^3\Pi)$), and O_3. Because of short life time of atomic oxygen and nitrogen, they cannot be detected by the mass spectroscopy system. The excited metastables show the same characteristics as their ground states in mass spectra and cannot be distinguished. Ozone will be decomposed by the ionization source in the mass spectrometer, and thus O_3 effect on the final spectra is almost negligible. Therefore, mass spectrometry is only effective for the analysis of nitrogen oxides in the afterglow of the jet. To quantify the yield of NO, a known premixed gas mixture of NO/dry air is used to calibrate the mass-spectrometer.

III. RESULT AND DISCUSSION

A. Electrical properties of the discharge

An application of high voltage to the electrodes leads to breakdown of the gas and formation of plasma. The main electron involved reactions in the active zone of N_2 plasma include nitrogen ionization $N_2 + e \rightarrow N_2^+ + 2e$, formation of nitrogen metastables: $N_2 + e \rightarrow N_2$ ($A^3\Sigma$, $B^3\Pi$, $C^3\Pi$)+e and electron impact dissociation with generation of atomic N in the states ^4S, ^2D, and ^2P (Paschen notation).[18] Ionization of O_2, $O_2 + e \rightarrow O_2^+ + 2e$, plays an important role in the sustainment of plasma in air. The electron attachment in the three body reactions $2O_2 + e \rightarrow O_2^- + O_2$ with a cross-section of 1.3×10^{-18} cm^2, $O_2 + e + N_2 \rightarrow O_2^- + N_2$ and the reaction of dissociative attachment $O_2 + e \rightarrow O + O^-$ starts to be the main mechanism of electron losses in air plasma.[19] The presence of O_2 results in the generation of atomic oxygen because of the electron impact dissociation

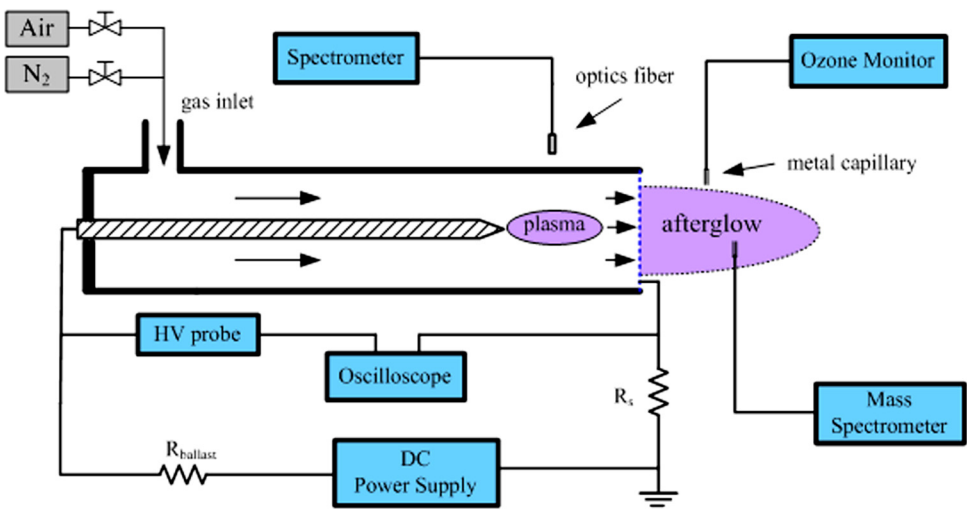

FIG. 1. Scheme of the DC plasma jet operating in N_2 or dry air.

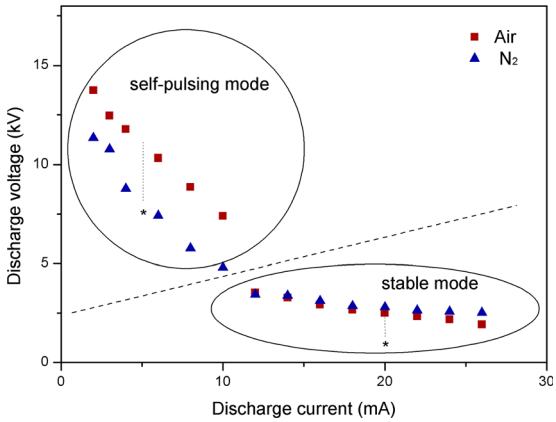

FIG. 2. Time average voltage/current characteristic of N_2 and air discharge. Position where images of the discharge have been taken are indicated with (*) marks.

reactions (1) and (2) and excited molecular oxygen by the reactions (3) and (4):[18,20]

$$O_2 + e \rightarrow O(^3P) + O(^3P) + e, \quad (1)$$

$$O_2 + e \rightarrow O(^3P) + O(^1D) + e, \quad (2)$$

$$O_2 + e \rightarrow O_2(a^1\Delta) + e, \quad (3)$$

$$O_2 + e \rightarrow O_2(b^1\Sigma) + e. \quad (4)$$

Self-sustainment of the DC jet is determined by equivalence of the ionization and recombination processes and leads to the current density: $J = n_e e \nu_e$. The average voltage-current characteristics of the N_2 plasma and air plasma are presented in Fig. 2. For both working gases (N_2 and air), there are two working modes depends on the discharge current. In the self-pulsing mode, the V/I characteristic has a negative slop. A change for slope is observed when the discharge is transferred to the glow-like stable mode at a discharge voltage and current of 4 kV and 10 mA, as shown in Figs. 2 and 4(b). In this stable mode, weak negative slope indicates that the discharge voltage slightly depends on the discharge current for both gases. The sharp increase in current in this region with a slow change in voltage corresponds to the formation of stable and diffuse plasma without oscillation of the current. The phenomenon of mode changing also has been observed for underwater dc discharge.[21] Both modes are also different in visual appearance.

Typical images of the plasma jet in N_2 and air are presented in Fig. 3. At a low average current, the discharge consists of a narrow filament with a pink or salmon color and with a diameter of 0.1–0.3 mm moving around cathode tip. Increase of the current to 10 mA results in the formation

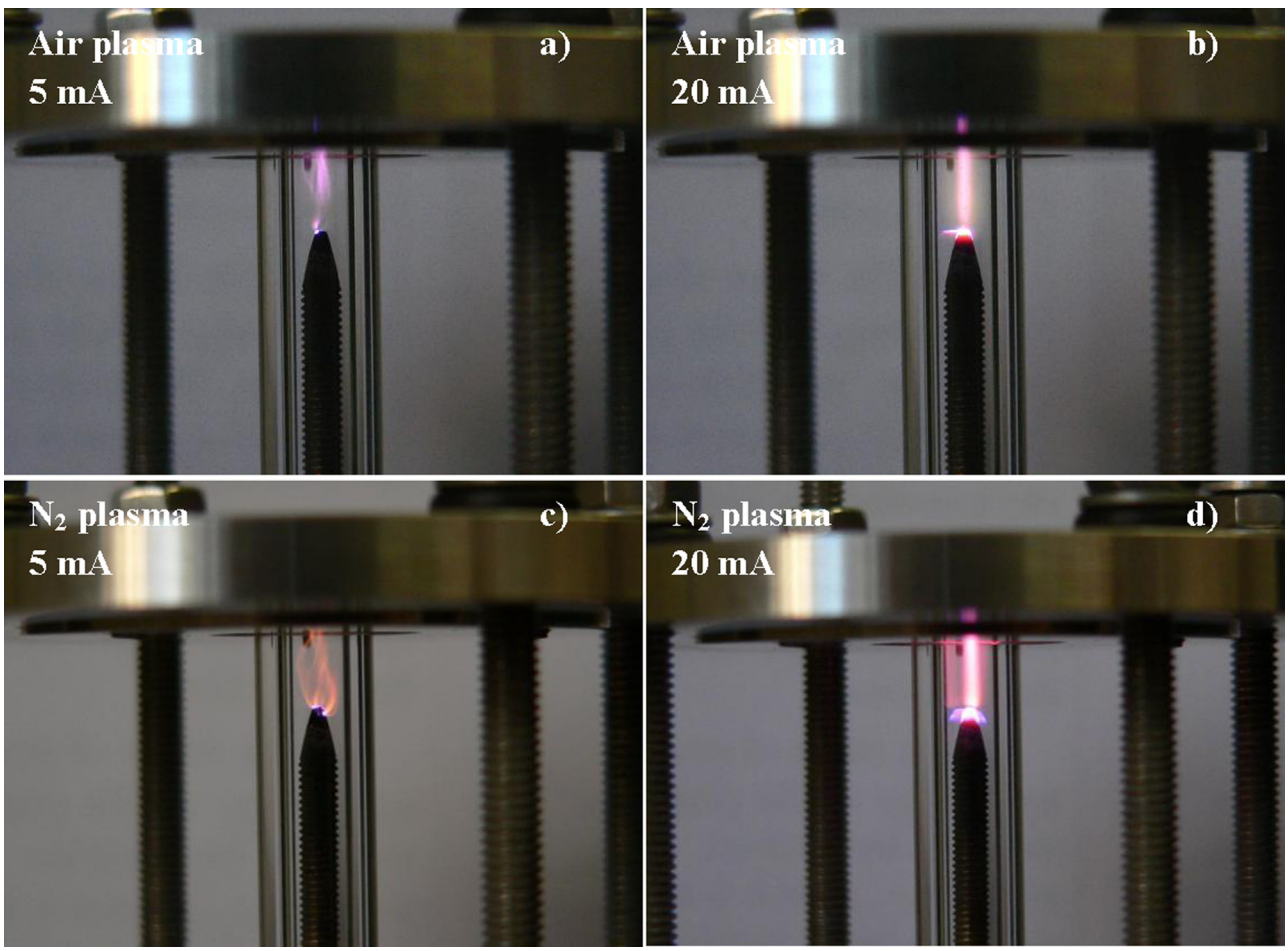

FIG. 3. Visual view of the discharge in air at current of 5 mA (a) and high current of 20 mA (b); discharge in N_2 at 5 mA (c) and 20 mA (d).

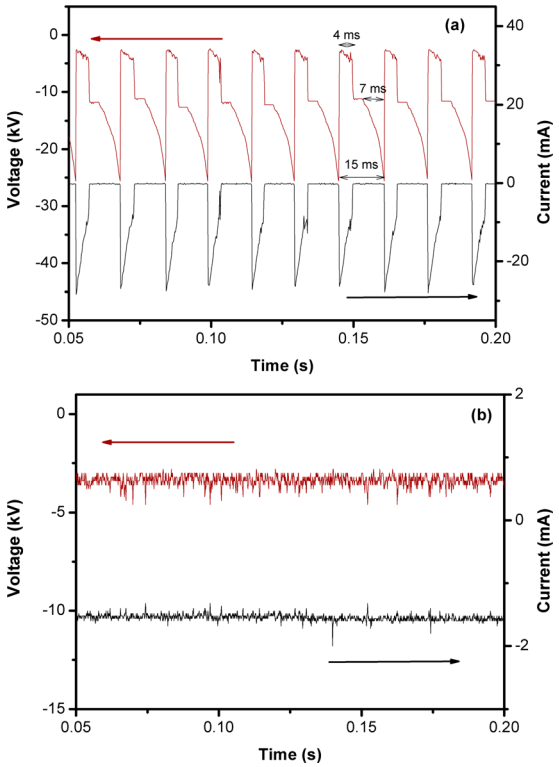

FIG. 4. Voltage, current waveforms in N_2 plasma in self-pulsing (a) and stable regimes (b) at average current of 5 mA and 15 mA, respectively.

of a diffuse plasma with a blue glowing region of 1–3 mm close to the tip of the cathode. At the highest achievable current of 30 mA, the discharge diameter is almost equal to the inner diameter of the quartz tube and filaments are not visible anymore. For a gas with a known electron mobility, an estimation of the discharge diameter allows us to determine the concentration of the electrons from $J = n_e e \nu_e = n_e e \mu_e E$, where J is the current density 15.3 A/cm^2 at 30 mA, e is the elementary charge, E is the electrical field in V cm^{-1}, and μ_e is the electron mobility in nitrogen or air. Accordingly, the electron density in the active zone of the nitrogen jet (current 30 mA) is estimated at 1.3×10^{21} m^{-3}, whereas it is 1.1×10^{21} m^{-3} in air due to the slightly higher electron mobility in air. At low discharge current, the expected electrons density should be higher because of the constriction of the discharge into narrow filaments. At low current level (< 5 mA), the discharge is sustained in a form of short current pulses with a duration of about 15 ms, as shown in Fig. 4(a). Since the voltage-current waveforms of nitrogen plasma and air plasma are similar to each other, only the typical waveforms of nitrogen plasma are presented in Fig. 4. Time resolved measurement reveals that the voltage applied on the electrodes drops from −12 kV to −4 kV after a slow decline to −8 kV, appearing during 4 ms. After a short period of 3–4 ms during which the voltage is constant, it decreases again until the moment when the breakdown stops. The frequency of the regular self-pulsing mode is determined by the RC time of the electrical circuit. Increasing the average current (more than 10 mA) generates a glow discharge with constant current and voltage, as shown in Fig. 4(b).

B. Diagnostics of the active zone of the discharge

1. Overview of the emission spectra

Diagnostics of the plasma active zone has been carried out by means of optical emission spectroscopy (OES). OES is the most common technique used in plasma diagnostics, especially in the UV-visible region for determining vibrational and rotational distribution functions of electronically excited states in molecular plasmas.[22,23] Typical survey spectra between 250 nm and 800 nm in the plasma regions for N_2 discharge and air discharge are shown in Figs. 5(a) and 5(b), respectively. The spectrometer used in the measurements is calibrated by standard tungsten ribbon lamps. Both plasmas are generated at 14 mA current, which means a stable mode of the discharge (Fig. 2). In N_2 and air discharge, the emission of the second positive system of the nitrogen molecule (N_2 ($C^3\Pi_u$-$B^3\Pi_g$), 281.4 nm–497.6 nm), the first negative system of the nitrogen molecular ion (N_2^+ ($B^2\Sigma_u$-$X^2\Sigma_g$), 329.3 nm–586.5 nm), and first positive system of the nitrogen molecule (N_2 ($B^3\Pi_g$-$A^3\Pi_u$), 503.1 nm–800 nm) are the main contributions to the spectra. Besides nitrogen vibrational emission, the nitric oxide γ-system (NO ($A^2\Sigma$ - $X^2\Pi$), 250–300.8 nm) is observed only for the plasma in air. In comparison with the N_2 plasma, the emitted intensity from the vibrational transitions N_2 ($B^3\Pi_g$ - $A^3\Pi_u$) and N_2^+ ($B^2\Sigma_u$ - $X^2\Sigma_g$) is lower in air plasma.

According to Akishev,[16] the vibrationally excited molecules determine the excitation and de-excitation processes in low-current discharge. For the discharge at current greater

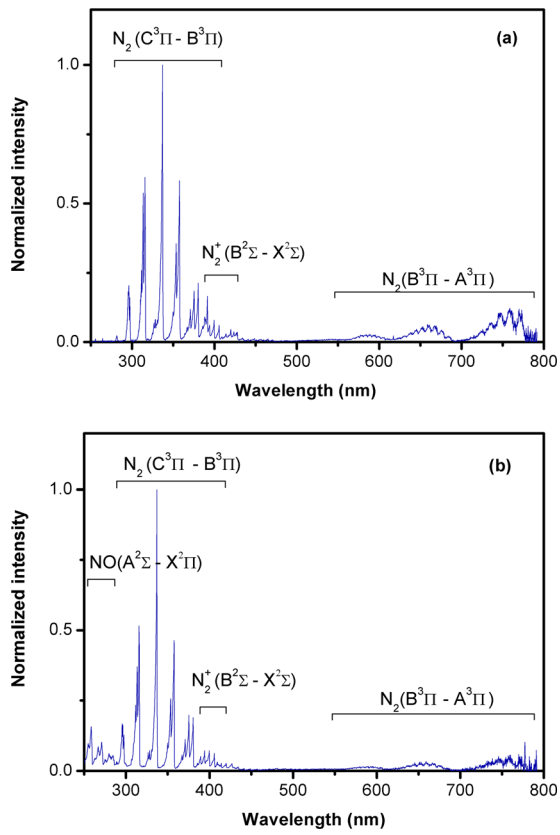

FIG. 5. A comparison of the emission spectra of DC discharge at air flow and nitrogen flow. (a) Plasma generated by nitrogen discharge at 14 mA; (b) plasma generated by air discharge at 14 mA.

than 10–15 mA, the energetic electrons and interparticle collision processes play a more important role in the dynamic balance of the charged species and excitation processes in plasma. The intensive N_2 molecular bands in the spectra indicate that discharge generates abundant metastable electronic excited nitrogen molecules and ionized species, such as $N_2(A)$, $N_2(B)$, $N_2(C)$, $N_2(a)$, and N_2^+.[16,24,25] Due to the relatively low excitation energy (6.17 eV), direct electron impact excitation by reaction (5) and the collisions between vibrational nitrogen molecules by reaction (6) contribute to the population of the excited state $N_2(A)$:

$$e + N_2(X^1\Sigma_g^+) \rightarrow N_2(A^3\Sigma_u^+) + e, \quad (5)$$

$$N_2(\nu_1) + N_2(\nu_2) \rightarrow N_2(A^3\Sigma_u^+) + N_2(X^1\Sigma_g^+). \quad (6)$$

Besides direct electron impact excitation and the collisions between vibrational nitrogen molecules, the excited state $N_2(B)$ is partly populated by the pooling reaction of the metastable state $N_2(A)$. From the spectra of both discharges, the strongest emission is observed at the second positive system of nitrogen N_2 ($C^3\Pi_u$ - $B^3\Pi_g$) which means the mechanism of the excitation process for $N_2(C)$ is mainly the direct electron impact excitation and the pooling reaction of the nitrogen metastable state

$$N_2(A^3\Sigma_u^+) + N_2(A^3\Sigma_u^+) \rightarrow N_2(C^3\Sigma_u) + N_2(X^1\Sigma_g^+). \quad (7)$$

2. Vibrational and rotational temperature measurements

The overpopulation of N_2 vibrational states indicates a high vibrational temperature (T_{vib}) of N_2 species. Three vibrational bands, $\Delta\nu = 1$ (1-0, 2-1, 3-2), $\Delta\nu = -1$(0-1, 1-2, 2-3), and $\Delta\nu = -2$ (0-2, 1-3, 2-4) are used in the Boltzmann plot method. The wavelengths and transition probabilities of each vibrational transition are listed in Table I.

A typical Boltzmann plot of the relative intensity distribution levels for the second positive system N_2 ($C^3\Pi_u$-$B^3\Pi_g$) is plotted in Fig. 6(a). The gas temperature in the active plasma zone (in the interelectrode gap) of the DC plasma jet is determined by analysis of the rotational structure of a nitrogen molecular band in the second positive system, namely the 0-0 vibrational band of N_2 ($C^3\Pi_u$-$B^3\Pi_g$)

TABLE I. Vibrational transitions of N_2 ($C^3\Pi_u$-$B^3\Pi_g$) for vibrational temperature.[26]

Sequence $\Delta\nu = \nu' - \nu''$	Vibrational transition $\nu' - \nu''$	Wavelength λ (nm)	Transition probability $A_{\nu'\nu''}$ (10^6 s^{-1})
+1	1-0	315.8	10.27
+1	2-1	313.5	8.84
+1	3-2	311.5	5.48
−1	0-1	357.6	7.33
−1	1-2	353.6	4.61
−1	2-3	349.9	1.46
−2	0-2	394.2	2.94
−2	1-3	399.7	4.10
−2	2-4	405.8	3.37

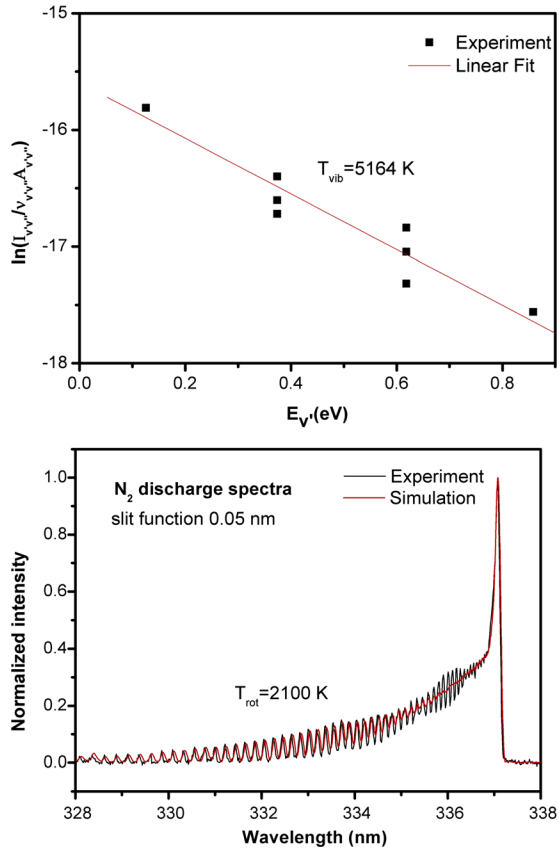

FIG. 6. (a) Typical Boltzmann plot of N_2 vibrational distribution. Three vibrational band series are chosen: $\Delta\nu = 1$ (1-0, 2-1, 3-2), $\Delta\nu = -1$(0-1, 1-2, 2-3), and $\Delta\nu = -2$ (0-2, 1-3, 2-4); (b) Determination of gas temperature by fitting procedure of experimental spectrum with calculated spectrum of N_2 ($C^3\Pi_u$-$B^3\Pi_g$, 0-0). The plasma is generated in nitrogen flow at 14 mA

emission at $\lambda = 337.1$ nm. The synthetic spectrum is calculated by Specair 2.2 program. A typical fitting procedure of the spectra for nitrogen plasma at 12 mA is presented in Fig. 6(b). For both air plasma and nitrogen plasma, Fig. 7 shows the results of the gas temperature T_{gas} and the vibrational temperature T_{vib} as a function of the discharge current. The vibrational temperatures T_{vib} for both discharges are much higher than the gas temperatures T_{gas}, which suggest a strong deviation from thermal equilibrium plasma. Compared to N_2

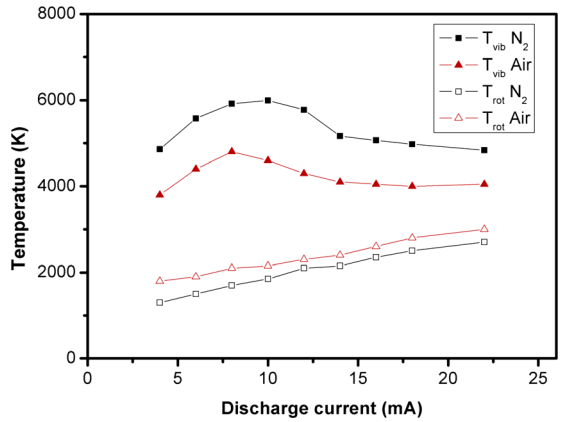

FIG. 7. Rotational and vibrational temperature in the active zone of the nitrogen and air discharge for different discharge current. Error of T_{vib} is in the range of ±200 K and for gas temperature is about ±50 K.

plasma, air plasma has a low vibrational temperature T_{vib} and a high gas temperature T_{gas}. The gas temperature of air plasma is approximately 300 K higher than the one of nitrogen plasma. Considering the high oxygen content of 21% in dry air, this heating effect is probably explained by a more effective energy transfer from electrons to molecular O_2 through excitation of vibrational and rotational levels of oxygen, which leads to the heating of the gas due to effective energy relaxation processes in the presence of O_2.[27] Both T_{vib} and T_{gas} strongly depend on the discharge current. T_{gas} is linearly increasing from 1300 K to 2750 K (N_2 plasma) and from 1750 K to 3000 K (Air plasma) at nearly the same slope rate with an increase of the current from 4 mA to 30 mA. T_{vib}, however, presents a nonlinear relationship with discharge current for both discharges. For air discharge, T_{vib} reaches a peak value of 4800 K at 8 mA and slightly drops to 4100 K at the maximum current. In N_2 plasma, the current for maximum T_{vib} (6050 K) is shifted to 10 mA and T_{vib} decreases to about 4800 K at highest current (30 mA). The approach of T_{vib} towards T_{rot} at high current indicates the thermalization of the discharge and the transformation of glow to arc plasma.

C. Diagnostics of the afterglow of the DC jet

1. Emission spectroscopy of the discharge afterglow

A distinguished advantage of an atmospheric pressure plasma jet is the fact that the available plasma volume is not limited to the gap between the electrodes. Besides the chemical reactive radicals and the metastable molecules generated in the discharge and blown out, species with long life time, e.g., O_3, can be formed in the afterglow of the jet. Typical survey spectra of the afterglow are presented in Fig. 8. The spectrum of the afterglow of N_2 discharge (Fig. 8(a)) shows similarities with one measured in the active zone (Fig. 5(a)), with only a difference in band intensities. On the other hand, a remarkable difference is observed between the spectra of afterglow and the ones of the active zone in air plasma, see Figs. 8(b) and 5(b). The strongest bands of the air jet in the active zone and the afterglow are dominated by the N_2 emission and NO emission, respectively. There is no NO emission in the spectra of the N_2 plasma afterglow. The behavior of the most intensive bands is presented for both plasmas as a function of discharge current in Figs. 9(a) and 9(b).

Based on OES results, it can be assumed that the afterglow of the N_2 jet mostly consists of N_2 metastables that are formed in the active zone and transported to the afterglow because of a sufficiently long life time. This is confirmed by Fig. 9(a), where the non-linear increasing of the bands intensities with increasing of the current correlates with the results of the vibrational temperature measurements in the active zone, see Fig. 7 for N_2 with the maximum of T_{vib} around 10 mA current. The main difference between active zone and afterglow of air plasma is the increase of the NO bands intensity in the afterglow of the former. We have to note that the vibrational temperature of the species in the afterglow of the N_2 plasma is higher than in the afterglow of air plasma. The former is about 3600 K at 6 mA, furthermore increases

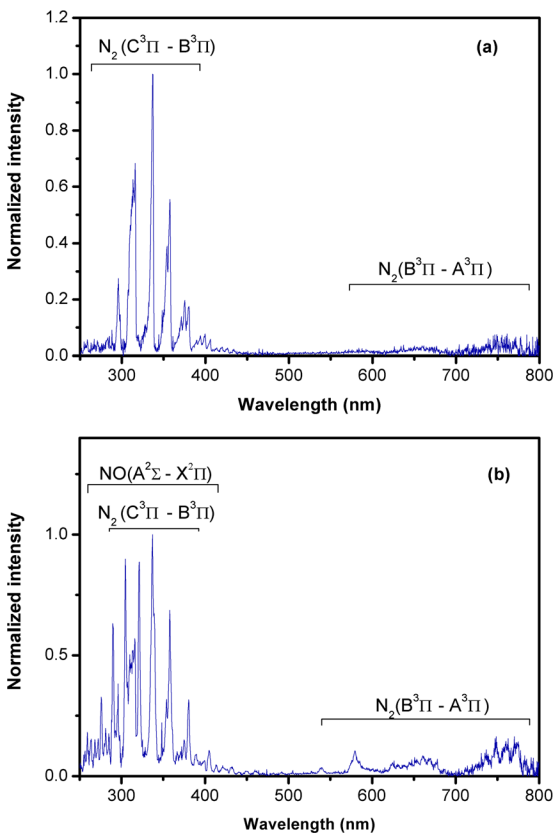

FIG. 8. Emission spectra of the afterglow (5 mm above the nozzle) of nitrogen (a) and air (b) discharge. Plasma generated at 14 mA and flow rate is 8 slm.

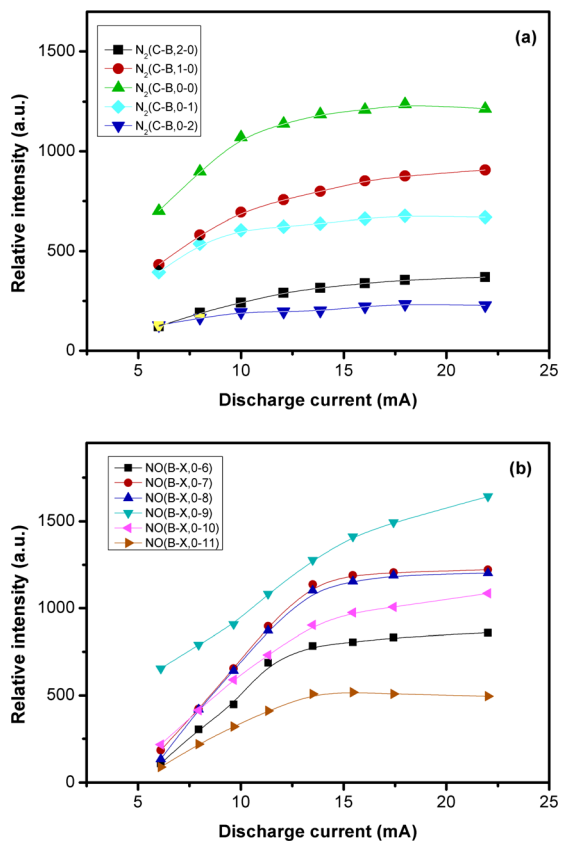

FIG. 9. The relative intensity of the strongest bands in N_2 (a) and air (b) as a function of the discharge current.

to 4600 K in the current range of 14–18 mA and then drops to 4200 K at 25 mA. At the same time, T_{vib} of air plasma afterglow does not exceed 1800 K. From a technological point of view for biomedical treatment, the used plasma source has to satisfy requirement of low gas temperature of the afterglow along with the high deviation from thermal equilibrium. The spatial resolved gas temperature measurements have been carried out with 1 cm resolution by the same technique as in part 3.2.2 and the results are presented in Figs. 10(a) and 10(b). The temperature of the gas drops down from 2000 K in the active zone to almost room temperature in the afterglow of both plasmas on the distance of 1 cm from the nozzle. This decrease is observed mainly due to the mixing with surrounding air and due to the heat transfer to the metal grid placed at the end of the nozzle. The decrease of the temperature in air plasma afterglow is smoother, which agrees with a fact that air plasma is closer to thermal equilibrium.

2. Mass-spectroscopy of NO and ozone monitoring

In the present study, diagnostics of the afterglow have been focused on long living species, especially the two species NO and O_3, which are considered to be important in biomedical applications of plasma jets. For air plasma, the evidence of NO generation in the active zone is confirmed by the emission from the nitric oxide γ-system NO ($A^2\Sigma$ - $X^2\Pi$) transition in the UV range. NO in the ground state is measured by mass-spectroscopy with preliminary calibration. A typical mass-spectrum of air plasma is presented on Fig. 11(a), together with spatially resolved NO measurements along the gas flow in the afterglow region, Fig. 11(b). Mass-spectroscopy shows only one new stable component—NO in the afterglow of the air discharge. The maximal achievable density of NO is about 1080 ppm at a current of 25 mA. NO concentration is decreasing linearly with the decline of the discharge current. The decrease of the NO concentration in the afterglow is mainly explained by dilution of the feed gas inasmuch as NO is formed in the active zone of the discharge. Nitrogen oxide is not observed in the afterglow of the N_2 plasma even at the highest current of 30 mA. In the discharge area, the electron impact dissociation of N_2 and O_2 molecules leads to the formation of atomic oxygen (reactions 1–3) and the breaking of the strong bond in the N_2 molecule by vibrational excitation and dissociation. Effective generation of NO in air plasma can be explained by so-called thermal NO through the Zel'dovich reactions[20,28]

$$N + O_2 \rightarrow NO + O(^3P), \tag{8}$$

$$N_2 + O \rightarrow NO + O(^3P), \tag{9}$$

which leads to formation of NO with consumption of atomic N or O. The NO yield has strong a temperature dependence and the NO generation is intensively reduced at $T_g < 2000$ K. NO in the ground state can also be formed in case of

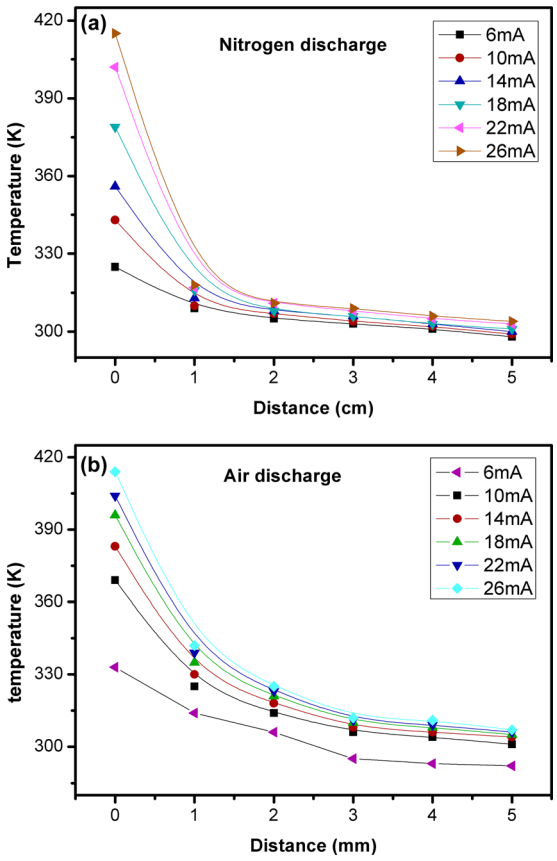

FIG. 10. Spatial distribution of the gas temperature in the discharge afterglow for (a) N_2 discharge; (b) air discharge. Error of the measurements is about 50 K.

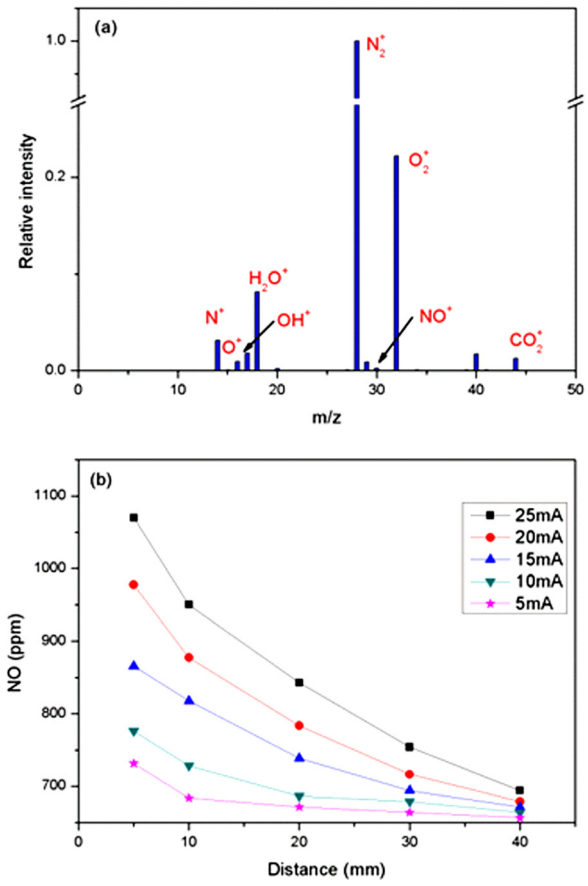

FIG. 11. (a) Mass-spectra of the air discharge afterglow (discharge current 14 mA); (b) spatially resolved NO measurements along the gas flow as a function of the discharge current.

non-equilibrium plasma by reactions (10) and (11) involving atomic nitrogen

$$O_2(b^1\Sigma) + N \rightarrow NO + O(^3P), \quad (10)$$

$$N(^2D,^2P) + O_2 \rightarrow NO + O(^3P,^3D). \quad (11)$$

The excited state of NO, on the other hand, is mainly provoked by nitrogen and oxygen metastable states, such as $N_2(A^3\Sigma)$, $N_2(B^3\Sigma)$, $O_2(a^1\Delta)$, $O_2(b^3\Sigma)$,[20,25] as in reactions (12) and (13)

$$N_2(A^3\Sigma, B^3\Sigma) + NO \rightarrow N_2 + NO, \quad (12)$$

$$O_2(a^1\Delta, b^3\Sigma) + NO \rightarrow O_2 + NO. \quad (13)$$

We expect the reason for the absence of NO in the N_2 plasma jet is the low dissociation degree of N_2 in the afterglow due to reaction (8). Therefore, the yield of NO by reactions (8), (10), and (11)) is negligible. At the same time, generation of NO in the active zone as in air discharge is impossible due to the absence of oxygen. In contrast to air plasma, a high density of O_3 is observed in the afterglow of N_2 discharge. The spatial distribution of O_3 in the afterglow of N_2 discharge is presented in Fig. 12.

The mechanism of ozone generation at high pressure is dominated by three-body processes, i.e., reactions[25]

$$O + O_2 + O_2 \rightarrow O_3 + O_2, \quad (14)$$

$$O + O_2 + N_2 \rightarrow O_3 + N_2. \quad (15)$$

This shows that ozone generation in the plasma mainly depends on the generation of atomic oxygen. The contribution of N_2 discharge to O_3 formation is mostly due to the formation of O atoms by atomic nitrogen and electronically excited nitrogen molecules. According to Ref. 20, the contribution of N atoms can take up about 10% to the total production of atomic oxygen and hence ozone generation. The most significant contribution to the formation of atomic oxygen, and thus ozone, is caused by the reactions of electronically excited nitrogen molecules

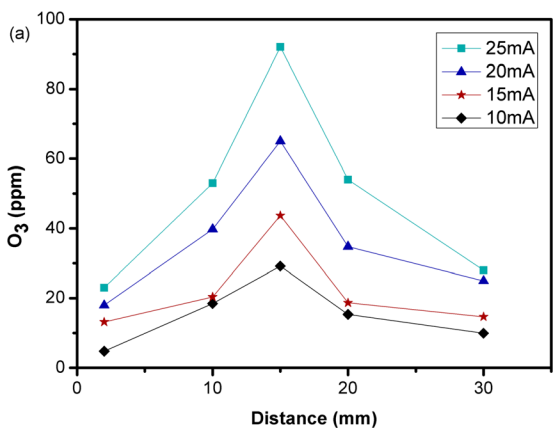

FIG. 12. The distribution of O_3 along the afterglow as a function of the current for N_2 discharge.

$$N_2(A^3\Sigma) + O_2 \rightarrow N_2(X^1\Sigma) + O + O, \quad (16)$$

$$N_2(B^3\Sigma) + O_2 \rightarrow N_2(X^1\Sigma) + O + O. \quad (17)$$

There are two main reasons for the absence of ozone in the afterglow of air discharge. First, a high concentration of nitrogen oxides completely stops the generation of O_3 by means of the discharge poisoning effect, which is related to fast reactions of O atoms with NO by the mechanism $O + NO + M \rightarrow NO_2 + M$. When the NO concentration exceeds the threshold value with about 0.1%, the reaction of atomic oxygen with nitrogen becomes faster than reactions with molecular oxygen, with the formation of ozone.[20] Second, the gas temperature in the active zone of air plasma is too high and thermal dissociation of O_3 starts to play an important role. So, even if ozone molecules already formed in the discharge, they will dissociate.

IV. CONCLUSION

The DC plasma jet in N_2 and air flow is investigated in terms of electrical parameters and efficiency of active species generation in the afterglow. Depending on the discharge current, two modes of plasma sustainment are determined. At a low average current $I < 5$ mA, the discharge is sustained in self-pulsing regime and at a current higher than 10 mA, the plasma behaves as a glow discharge without oscillations of the voltage and current. Vibrational and gas temperature of the plasma jet are determined from emission spectroscopy for the active zone and the afterglow. The vibrational temperatures T_{vib} for both discharges are much higher than the gas temperatures T_{gas}, which indicates that the plasmas are far away from thermal equilibrium. A stronger deviation from thermal equilibrium in N_2 plasma is indicated by higher T_{vib} and lower T_{gas}. The use of air (21% O_2) results in the decrease of T_{vib} and the increase of T_{gas} in comparison with N_2 discharge. It is revealed that T_{vib} and T_{gas} strongly depend on discharge current. For both discharges, T_{gas} is linearly increasing from 1300 to 2750 K (N_2 plasma) and from 1750 to 3000 K (Air plasma) with the increase of current to 30 mA at nearly a same slope rate. However, T_{vib} of both discharges presents a nonlinear relationship versus discharge current. The approach of T_{vib} to T_{rot} at high current indicates the thermalization of the discharges and the transfer of glow to arc plasma. The afterglow of N_2 and air plasmas is characterized by a gas temperature almost equal to room temperature and still high (up to 4600 K in N_2 on 5 mm distance from the nozzle) vibrational temperature. The afterglow emission of the N_2 plasma jet is produced by N_2 metastables. The afterglow spectrum of air plasma jet is dominated by NO emission. The afterglow of plasma jets is characterized in terms of the production of long living species—O_3 and NO. NO is only detected in the air plasma jet at concentration up to 1100 ppm (25 mA current) and O_3 is only found in the afterglow of the N_2 plasma jet. The absent of O_3 in air jet is expected to be caused for two reasons: a high concentration of NO in the air plasma completely stops the generation of O_3 probably by means of the discharge poisoning effect,

and thermal dissociation of O_3 starts to play an important role due to the high gas temperature of the active zone.

ACKNOWLEDGMENTS

This work was supported by the China Scholarship Council (CSC) and Co-funding scholarship of Ghent University.

[1]N. De Geyter, R. Morent, T. Jacobs, F. Axisa, L. Gengembre, C. Leys, J. Vanfleteren, and E. Payen, Plasma Processes Polym. **6**, S406 (2009).
[2]R. Morent, N. De Geyter, S. Van Vlierberghe, P. Dubruel, C. Leys, L. Gengembre, E. Schacht, and E. Payen, Prog. Org. Coat. **64**, 304 (2009).
[3]S. Samukawa, M. Hori, S. Rauf, K. Tachibana, P. Bruggeman, G. Kroesen, J. C. Whitehead, A. B. Murphy, A. F. Gutsol, and S. Starikovskaia, J. Phys. D: Appl. Phys. **45**, 253001 (2012).
[4]K. D. Weltmann, E. Kindel, R. Brandenburg, C. Meyer, R. Bussiahn, C. Wilke, and T. von Woedtke, Contrib. Plasma Phys. **49**, 631 (2009).
[5]S. Wu, Z. Wand, Q. Huang, X. Lu, and Y. Pan, IEEE Trans Plasma Sci. **39**, 1489 (2011).
[6]E. Temmerman, Y. Akishev, N. Trushkin, C. Leys, and J. Verschuren, J. Phys. D: Appl. Phys. **38**, 505 (2005).
[7]Y. Akishev, O. Goossens, T. Callebaut, C. Leys, A. Napartovich, and N. Trushkin, J. Phys. D: Appl. Phys. **34**, 2875 (2001).
[8]J. Liebmann, J. Scherer, N. Bibinov, P. Rajasekaran, R. Kovacs, R. Gesche, P. Awakowicz, and V. Kolb-Bachofen, Nitric Oxide **24**, 8 (2011).
[9]P. Kouakou, V. Brien, B. Assouar, V. Hody, M. Belmahi, H. N. Migeon, and J. Bougdira, Plasma Processes Polym. **4**, S210 (2007).
[10]N. Masoud, K. Martus, M. Figus, and K. Becker, Contrib. Plasma Phys. **45**, 32 (2005).
[11]S. Kühn, N. Bibinov, R. Gesche, and P. Awakowicz, Plasma Sources Sci. Technol. **19**, 015013 (2010).
[12]R. Weller, Br. J. Dermatol. **137**, 665 (1997).
[13]C. V. Suschek, T. Schewe, H. Sies, and K. D. Kroncke, Biol. Chem. **387**, 499 (2006).
[14]I. E. Kieft, J. J. B. N. van Berkel, E. R. Kieft, and E. Stoffels, *Plasma Processes and Polymers* (Wiley VCH, Weinheim, 2005)
[15]Y. Akishev, M. Grushin, V. Karalnik, I. Kochetov, A. Napartovich, and N. Trushkin, J. Phys.: Conf. Ser. **257**, 012014 (2010).
[16]Y. Akishev, M. Grushin, V. Karalnik, A. Petryakov, and N. Trushkin, J. Phys. D: Appl. Phys. **43**(7), 075202 (2010).
[17]Y. Akishev, M. Grushin, V. Karalnik, A. Petryakov, and N. Trushkin, J. Phys. D: Appl. Phys. **43**(21), 215202 (2010).
[18]Y. Itikawa, M. Hayashi, A. Ichimura, K. Onda, K. Sakimoto, K. Takayanagi, M. Nakamura, H. Nishimura, and T. Takayanagi, J. Phys. Chem. Ref. Data **15**, 985 (1986).
[19]D. R. Bates, *Atomic and Molecular Processes* (Academic, New York, 1962).
[20]A. Fridman, *Plasma Chemistry* (Cambridge University Press, Cambridge, 2008).
[21]A. Y. Nikiforov, C. Leys, L. Li, L. Nemcova, and F. Krcma, Plasma Sources Sci Technol. **20**, 034008 (2011).
[22]E. Stoffels, A. Flikweert, W. Stoffels, and G. Kroesen, Plasma Sources Sci. Technol. **11**, 383 (2002).
[23]C. Laux, T. Spence, C. Kruger, and R. Zare, Plasma Sources Sci. Technol. **12**, 125 (2003).
[24]T. Callebaut, I. Kochetov, Y. Akishev, A. Napartovich, and C. Leys, Plasma Sources Sci Technol. **13**, 245 (2004).
[25]I. Kossyi, A. Y. Kostinsky, A. Matveyev, and V. Silakov, Plasma Sources Sci Technol. **1**, 207 (1992).
[26]D. E. Shemasky and A. L. Brroadfoot, J. Quant. Spectrosc. Radiat. Transf. **11**, 1385 (1971).
[27]E. M. Bazelyan and Y. P. Raizer, *Spark Discharge* (CRC, New York, 1998).
[28]S. C. Hill and L. D. Smoot, Prog. Energy Combust. Sci. **26**(4–6), 417 (2000).